Soft Matter

PAPER

Check for updates

Cyclodextrin-catalyzed self-assembly of a coordinating fluorescent molecule into microflowers†

Ting Gu, Jianbin Huang* and Yun Yan ⓘ *

We report that γ-cyclodextrin (γ-CD) is able to catalyze the self-assembly process of the coordinating fluorescent molecule pyrenebutyrate with Zn^{2+}. The direct interaction between pyrenebutyrate and Zn^{2+} would simply lead to amorphous precipitates, whereas addition of Zn^{2+} to the host–guest complex of pyrenebutyrate @ γ-CD would generate well-defined microflowers that have exactly the same composition as the amorphous pyrenebutyrate/Zn^{2+}. The evidence of host–guest formation between 1-PBA and γ-CD and the absence of γ-CD in the final microflowers manifest that γ-CD acts as a catalyst in the self-assembly process. We envision that this dynamic host–guest chemistry would be very promising in creating catassemblies.

Introduction

Chemical synthesis and molecular assembly are the two approaches leading to new materials. In chemical synthesis, catalysts play paramount roles. By definition, catalysts are substances that change the reaction rate while they do not change the Gibbs free energy of the total reaction. In principle, catalysts decompose one reaction step into several multi-steps through binding with the reactants to form an intermediate complex, thus decreasing the activation energy. In the scope of molecular self-assembly, the path and rate of assembly sometimes can also be modulated by catalysts. Tian *et al.* defined this phenomenon as catassembly and the catalyst leading to desired self-assembled structures as catassemblers.[1] To date, there are mainly two principles that explain how catassemblers work: (1) the catassembly processes are regulated by catassemblers through multi-site synergistic non-covalent interactions; (2) catassemblers interact with building blocks, modulating the whole systems' non-covalent interaction. The catassembly process has various merits like high efficiency and selectivity compared to their uncatalyzed counterparts. In the past decade, some extraordinary examples of catassembly were indeed reported.[2–7] However, the knowledge on catassembly is still very limited, and considerable efforts are highly desired to explore new catassemblers in different catassemblies.

*Beijing National Laboratory for Molecular Sciences (BNLMS), State Key Laboratory for Structural Chemistry of Unstable and Stable Species, College of Chemistry and Molecular Engineering, Peking University, Beijing, 100871, P. R. China.
E-mail: yunyan@pku.edu.cn, jbhuang@pku.edu.cn*

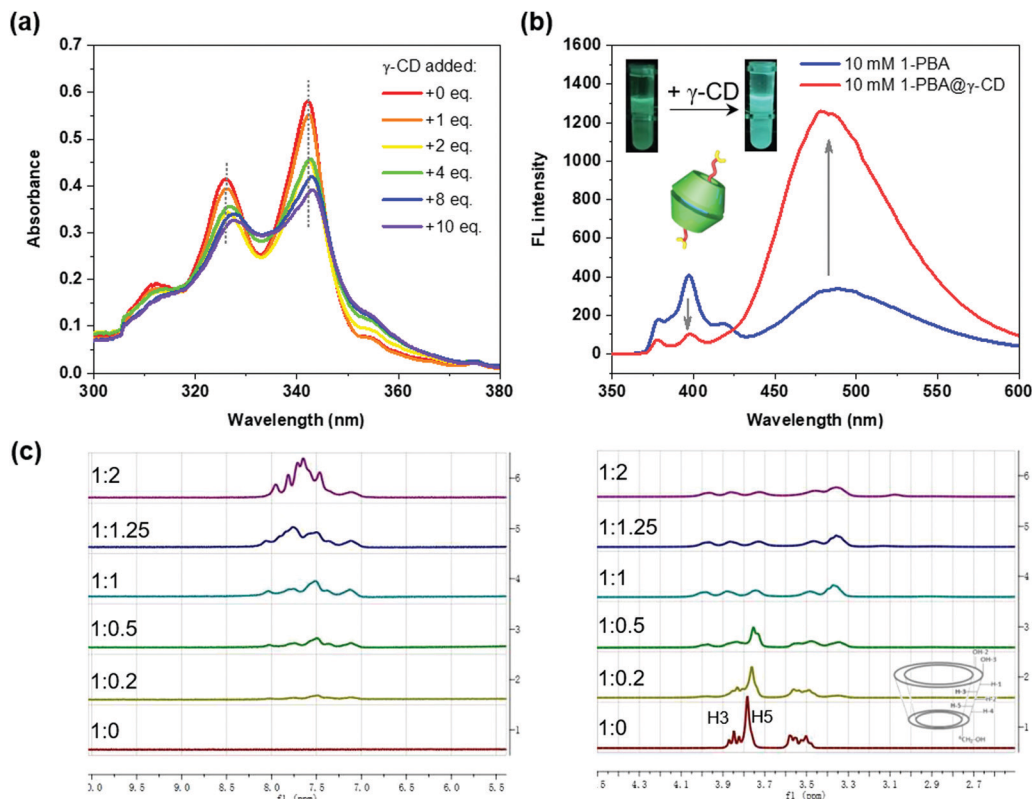† Electronic supplementary information (ESI) available. See DOI: https://doi.org/10.1039/d2sm00462c

In this paper, we report a case of γ-CD catalyzed coordinating self-assembly of microflowers with the fluorescent molecule 1-PBA and Zn^{2+} ions. We found that the host–guest interaction between γ-CD and 1-PBA is of paramount significance for the microflower formation, but there is no γ-CD in the microflowers. The chemical composition of the microflowers is exactly the same as that of the amorphous 1-PBA/Zn^{2+} precipitates. Different from other works utilizing CD as part of the building blocks to construct the final assembly,[8–13] CD in this work only participates in the intermediate assembly process and leaves the final coordinating self-assembly formed with 1-PBA and Zn^{2+}, and is therefore a typical catassembler. We envision that the dynamic and reversible characteristics of the host-guest chemistry of cyclodextrins may be very promising in designing more intriguing catassemblies.

Results and discussion

Pyrenebutyrate (1-PBA) is a pyrene derivative which has a butyl carboxylate at pyrene's 1' position. According to the size matching effect, it is expected that 1-PBA can be easily encapsulated in the cavity of γ-CD. The UV-Vis spectrum shows that upon addition of γ-CD into the 1-PBA solution, the monomer absorbance of the pyrene group at 340 nm keep decreasing, broadening and red shifting (Fig. 1a). These changes are characteristic of encapsulation of the pyrene group into γ-CD.[14,15] Moreover, the monomer emission decreases largely while the excimer emission at 480 nm is enhanced by nearly 3.5 times (Fig. 1b). This enhanced excimer emission indicates the formation of a pyrene dimer in the barrel-like cavity formed

Fig. 1 (a) UV-Vis spectrum using γ-CD to titrate 0.1 mM 1-PBA and (b) fluorescence emission spectrum of 10 mM 1-PBA and 10 mM 1-PBA@γ-CD (λ_{ex} = 310 nm). The insets are images of solutions under 365 nm UV lamp. (c) ^{1}H NMR (400 MHz, D$_2$O, 25 °C) spectra for the solution of γ-CD (5 mM) in the lower (left) and upper (right) field region titrated with 1-PBA. The γ-CD/1-PBA molar ratios are 1:0, 1:0.2, 1:0.5, 1:1, 1:1.25 and 1:2.

by two γ-CDs.[16–18] The formation of inclusion complexes between 1-PBA/γ-CD is further confirmed by ^{1}H NMR (Fig. 1c). The chemical shifts for the H3 and H5 protons of γ-CD have moved to a higher field upon addition of 1-PBA into γ-CD, accompanied by peak merging and broadening (Fig. 1c, right panel), which is characteristic of the ring current of the aromatic portion of 1-PBA that is included in the cavity.[19] The spectra for protons of γ-CD remain unchanged while that for the 1-PBA becomes sharper (Fig. 1c, left panel) when the amount of 1-PBA surpasses γ-CD, indicating that they bind in an equal molar pattern. Literature reports have confirmed that pyrene and its derivatives will form a 2:2 complex with γ-CD, and the equilibrium constants between 1-PBA and γ-CD have been obtained both theoretically and experimentally.[18,20] Here the encapsulation of the 1-PBA dimer into the cavity of γ-CD is further evidenced by the high-resolution MS (Fig. S1, ESI†).

It has been widely recognized that addition of metal ions into the solution of a coordinating amphiphile would lead to coordinating self-assembly.[21–24] Here Zn(NO$_3$)$_2$ was added dropwise into both the aqueous 1-PBA and the 1-PBA@γ-CD host–guest system. Both the two transparent solutions turned turbid immediately, and white precipitates were formed within a few seconds. SEM observation reveals that the precipitates in the 1-PBA system are amorphous (Fig. 2a), whereas those formed in the 1-PBA@γ-CD system are well-defined micro-flowers with the average diameter ∼5 μm (Fig. 2b). Elemental
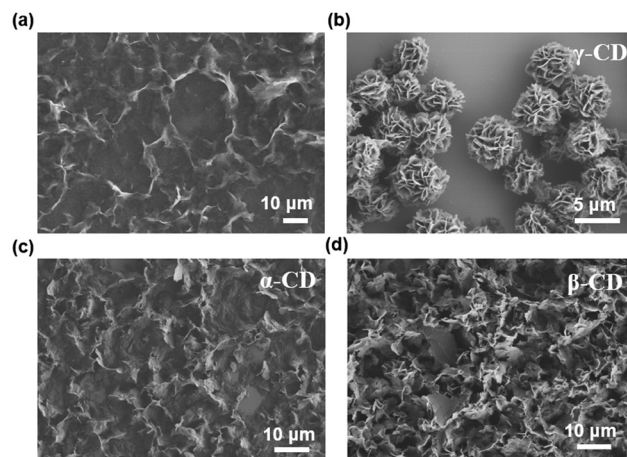

Fig. 2 SEM images of the precipitates obtained in different 1-PBA/Zn^{2+} systems: (a) without CD; (b–d) in the presence of equimolar of γ-CD, α-CD, and β-CD, respectively.

analysis indicates that both precipitates have nearly the same C, H and O contents (Table 1). The molar ratio of 1-PBA:Zn^{2+} is found to be 2:1, indicating that γ-CD does not exist in the microflowers, and both the amorphous precipitates and the microflowers have the chemical composition of Zn(1-PBA)$_2$.

FT-IR measurements were performed to reveal whether there are differences in the binding mode between 1-PBA and Zn^{2+} in

Table 1 Elemental analysis results of microflowers and amorphous precipitates

Samples	C (wt%)	H (wt%)	O (wt%)
Microflowers	70.31	5.02	14.22
Amorphous precipitates	70.82	5.54	14.07
$Zn(1\text{-}PBA)_2 \cdot 2H_2O$ (calculated)	71.11	5.04	14.22

the two precipitates. Usually, carboxylate acid displays a single band around 1700 cm^{-1} that arises from the antisymmetric C=O stretching. Upon coordinating with metal ions, this single band splits into doublet ones, corresponding to the asymmetric and symmetric stretching vibration of C=O, respectively. The frequency separation $\Delta\nu = \nu_{as}(COO^-) - \nu_s(COO^-)$ characterizes different coordinating modes between metal ions and carboxyl groups.[25–27] For the two precipitates, the IR spectra are similar, and the separation (77, 109 cm^{-1}) is far less than 200 cm^{-1}, suggesting bidentate chelating coordination in these precipitates (Fig. 3a). Furthermore, X-ray powder diffraction reveals that the diffraction peaks are almost overlapped for the two precipitates, but their intensities are drastically different (Fig. 3b). The diffraction of amorphous precipitates is very sharp and intense compared to the broadened and weak features of the microflowers, indicating that the $Zn(1\text{-}PBA)_2$ unit in both the amorphous precipitates and the

microflowers packed in the same way, but the periodical nature in the amorphous precipitates is more significant. It is noticed that the XRD pattern of both precipitates gives diffractions at $2\theta = 3.31°$, $6.66°$, $10.00°$ and $13.37°$. The corresponding spacing ratio is $1:2:3:4$, characterizing (100), (200), (300) and (400) Miller Indices of a 2D lamellar mesostructure.[28] According to the Bragg equation, the interlayer distance can be calculated from the (100) diffraction, which is 2.67 nm. Considering that the extending length of a pair of 1-PBA molecules bridged by one Zn^{2+} ion is about 2.6 nm (Fig. S2, ESI†), which is close to 2.67 nm calculated from the XRD results, the precipitates are inferred to be the stacking layers of the Zn^{2+} bridged two extending 1-PBA molecules. The stacking mode of the 1-PBA unit can be further inferred from the emission spectra, since the emission features of pyrene moieties correlate closely to their stacking pattern.[14–16] Compared to monomer emission, the emission peaks for the amorphous precipitates and microflowers are both broad and red-shifted. Meanwhile, the fluorescence lifetime has been shortened (Fig. 3c and d), which is characteristic of pyrene excimers.[16,29] This means that 1-PBA molecules are packed in a face-to-face fashion in both systems. Under CLSM, the microflowers can be clearly observed (Fig. S3, ESI†). Quantum yield measurement reveals that the quantum yield of the microflowers is 12.3%, which is approximate to that of the amorphous precipitates of 13.6% (Fig. S4, ESI†).
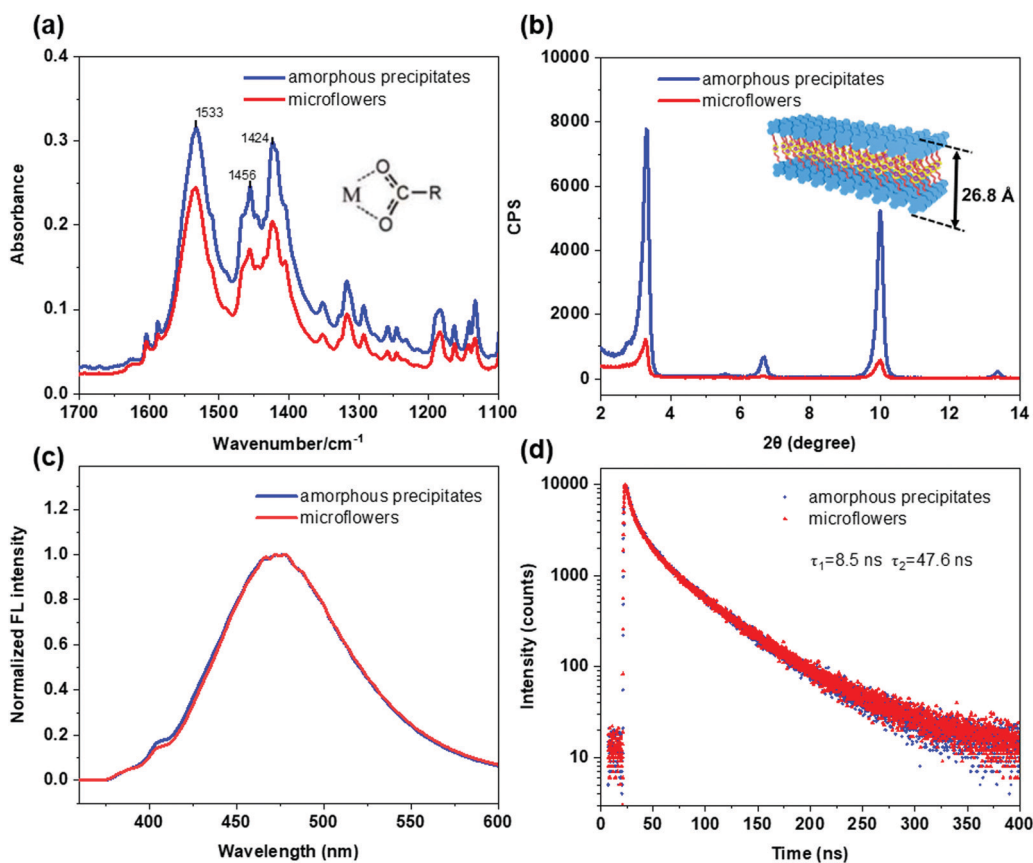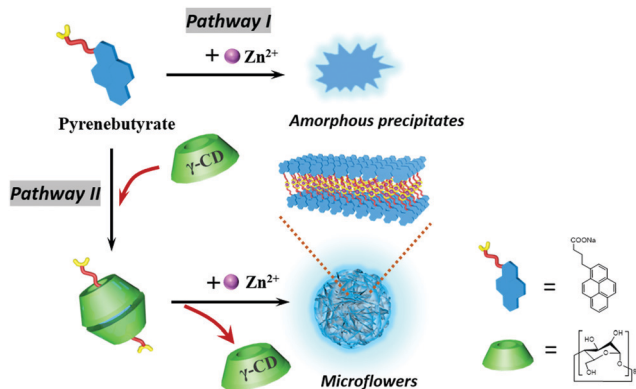

Fig. 3 (a) IR, (b) XRD analysis, the inset is the proposed molecule stacking pattern in the aggregates, (c) emission spectra (λ_{ex} = 340 nm) and (d) fluorescence decay profiles of the two precipitates.

Scheme 1 Schematic drawing of the proposed mechanism of γ-cyclodextrin catalyzed molecular self-assembly of pyrenebutyrate and Zn^{2+} into microflowers.

It is clear that formation of the host–guest complex of 1-PBA@γ-CD plays a determinative role in the generation of the microflowers. As γ-CD was replaced with α,β-CD, microflowers cannot be formed any more (Fig. 2c and d). UV-Vis and fluorescence titration experiments (Fig. S5, ESI†) reveal that neither α-CD nor β-CD is able to form a host–guest complex with 1-PBA. This is reasonable, since the cavity diameter of α-CD and β-CD is 0.57 nm and 0.78 nm, respectively, which is less

than or nearly the same as the width of pyrene (0.7 nm), thus making it difficult to form a host–guest complex between them.

The molar ratio between γ-CD and 1-PBA is also very critical for the microflower formation. It is revealed that when γ-CD is insufficient (0.5 equiv. of 1-PBA), a large amount of irregularly stacked sheets formed. In contrast, when γ-CD is in large excess, the morphology of the $Zn(1\text{-PBA})_2$ self-assembly transforms from microflowers into larger solid microspheres with a rough surface. The zoomed-in SEM image reveals that the microspheres are composed of densely-stacked sheets (Fig. S6, ESI†). The aforementioned results indicate that γ-CD has changed the building block that interacts with Zn^{2+}. Without γ-CD, the strong electronic attraction and coordination interaction between Zn^{2+} and the COO^- group of 1-PBA occur instantly, so that the amorphous precipitates are formed. However, as the 1-PBA is threaded into the cavity of γ-CD, the interaction between 1-PBA and Zn^{2+} occurs as well, but stacking of 1-PBA is hindered by γ-CD which hosts the 1-PBA. Stacking of 1-PBA becomes possible only when the γ-CD detaches from it in the process of host–guest dynamics. As a result, the stacking of 1-PBA is not as facile as that in the γ-CD free system, and the smaller flakes tend to integrate to microflowers to maximumly minimize the surface energy. The mechanism of the γ-CD catalyzed self-assembly of Zn/1-PBA is illustrated in Scheme 1.

It should be clarified that the role of γ-CD is not to reduce the effective concentration that is to interact with Zn^{2+}. Control
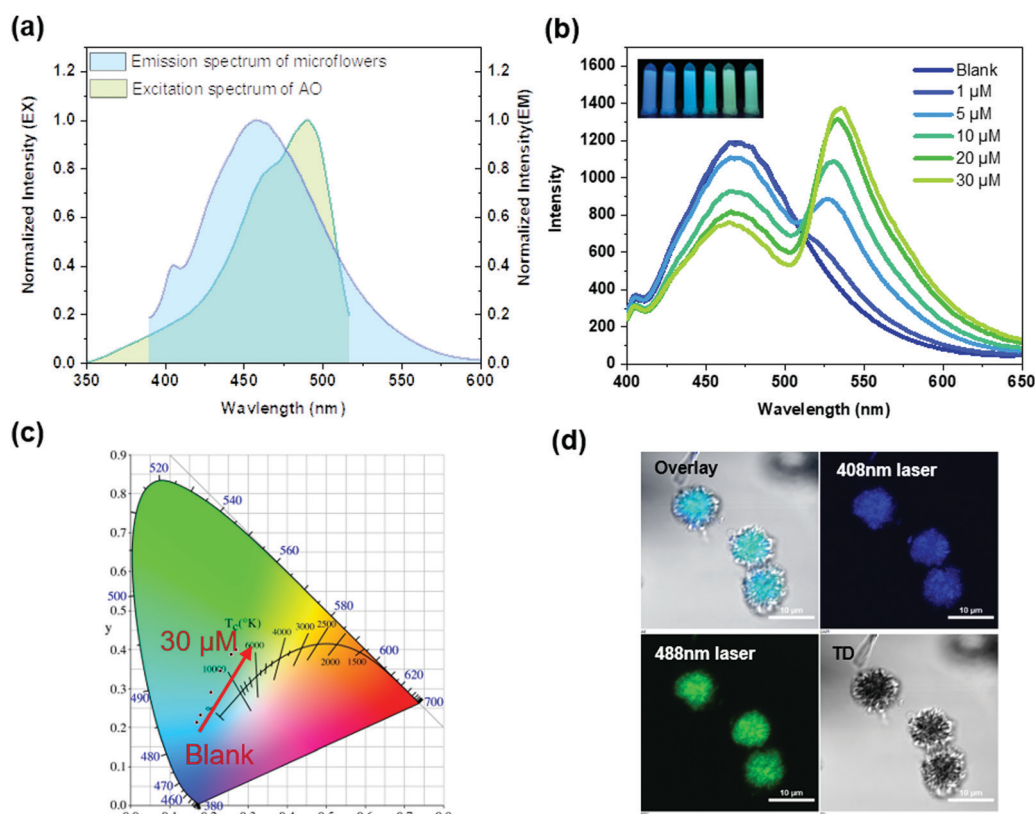

Fig. 4 (a) Emission spectrum of microflowers and excitation spectrum of AO, (b) fluorescence spectrum and (c) CIE coordinate diagram of microflowers adsorbing different amounts of AO dye excited at 370 nm, and (d) CLSM images of a representative sample.

experiments revealed that in the absence of γ-CD, neither lowering the concentration of 1-PBA nor varying the molar ratios between 1-PBA and Zn^{2+} would lead to the formation of microflowers (Fig. S7, ESI†). Actually, a critical concentration is required for the formation of microflowers. As the concentration of 1-PBA is below 4 mM, the petals of the microflower are not in contact (Fig. S8, ESI†), and prolonging the aging time would not affect the status of the microflowers. SEM observation revealed that the microflowers were formed immediately after the addition of Zn^{2+} and their size and morphology barely changed with time (Fig. S9, ESI†).

The microflowers and irregular precipitates have different specific surface area. The BET surface area of the microflowers is determined to be 49.2 m^{-2} g^{-1}, which is much higher than the value 8.8 m^{-2} g^{-1} of the amorphous precipitates (Fig. S10, ESI†). This means that the microflowers would have better adsorbing ability than the amorphous precipitates. According to zeta potential measurement, the surface of the microflowers carries negative charges, which is evidenced by the potential value of -28 ± 3.4 mV. Therefore, cationic fluorescent dyes like Rhodamine 6G (Rh6G), Thioflavin T (ThT) and Acridine Orange (AO) can be facilely adsorbed in the microflowers (Fig. S11, ESI†). Fig. 4 shows the design of a light-harvesting system by adsorbing AO on the microflowers. Because the emission of 1-PBA overlaps well with the excitation band of AO (Fig. 4a), addition of AO to the suspension of the microflowers will lead to fluorescence energy transfer between 1-PBA and AO. Fig. 4b shows that as the concentration of AO increases from 0 μM to 30 μM, the emission of the microflowers at 470 nm is weakened gradually and the emission from AO at around 530 nm rises up accordingly. Good linear CIE coordinates are observed spanning from (0.169, 0.213) to (0.270, 0.399) (Fig. 4c). CLSM images showed that the adsorption of AO didn't change the morphology of the microflowers (Fig. 4d), indicating that the microflowers are robust in view of being used as functional materials.

In conclusion, we have demonstrated a strategy of utilizing host–guest interaction between γ-CD and 1-PBA to modulate the coordinating self-assembly pathway of 1-PBA with Zn^{2+}. Because of the formation of the host–guest complex between γ-CD and 1-PBA, the stacking of the $Zn(1\text{-PBA})_2$ would be disturbed by the detaching of γ-CD from 1-PBA. As a result, smaller petals composed of layered stacking of the $Zn(1\text{-PBA})_2$ unit would come into formation and they further pack into microflowers. Since the microflowers and the amorphous precipitates have exactly the same composition, γ-CD is thus acting as merely a catalyst that appears as an intermediate for the microflower formation. Compared with the amorphous precipitates, the microflowers have 5.6 times larger specific surface area and have enhanced adsorbing ability, and thus can be used to construct a light-harvesting system by adsorbing the acceptor dye of AO. We envision that the dynamic host–guest interaction can be very promising in constructing catassembly and improving the function of the self-assembled materials, as well as expanding the role of host–guest interaction in fabricating state-of-the-art materials.

Conflicts of interest

There are no conflicts to declare.

Acknowledgements

References

1 Y. Wang, H.-X. Lin, L. Chen, S.-Y. Ding, Z.-C. Lei, D.-Y. Liu, X.-Y. Cao, H.-J. Liang, Y.-B. Jiang and Z.-Q. Tian, *Chem. Soc. Rev.*, 2014, **43**, 399–411.

2 J. S. Zhao, J. H. Wang, W. B. He, Y. B. Ruan and Y. B. Jiang, *Chemistry*, 2012, **18**, 3631–3636.

3 H. Li, X. Xu, J. Shang, J. Li, X. Hu, B. K. Teo and K. Wu, *J. Phys. Chem. C*, 2012, **116**, 21753–21761.

4 L. J. Prins, F. De Jong, P. Timmerman and D. N. Reinhoudt, *Nature*, 2000, **408**, 181–184.

5 Y. Chen, J.-J. Liu, C.-R. Fan, J.-Q. Li and M.-J. Lin, *Sci. China: Chem.*, 2016, **59**, 1492–1497.

6 R. Lauceri, A. Raudino, L. M. Scolaro, N. Micali and R. Purrello, *J. Am. Chem. Soc.*, 2002, **124**, 894–895.

7 L. Zhao, L. Jiang, Y. Han, Z. Xian, J. Huang and Y. Yan, *Soft Matter*, 2013, **9**, 7710–7717.

8 Y. Wang, N. Ma, Z. Wang and X. Zhang, *Angew. Chem., Int. Ed.*, 2007, **46**, 2823–2826.

9 K. Liu, C. Ma, T. Wu, W. Qi, Y. Yan and J. Huang, *Curr. Opin. Colloid Interface Sci.*, 2020, **45**, 44–56.

10 L. Szente and É. Fenyvesi, *Struct. Chem.*, 2016, **28**, 479–492.

11 A. Harada and M. Kamachi, *Macromolecules*, 1990, **23**, 2821–2823.

12 R. A. Smaldone, R. S. Forgan, H. Furukawa, J. J. Gassensmith, A. M. Slawin, O. M. Yaghi and J. F. Stoddart, *Angew. Chem., Int. Ed.*, 2010, **49**, 8630–8634.

13 Y. Chen, Y. M. Zhang and Y. Liu, *Chem. Commun.*, 2010, **46**, 5622–5633.

14 J. J. Li, H. Y. Zhang, G. Liu, X. Dai, L. Chen and Y. Liu, *Adv. Opt. Mater.*, 2020, **9**, 2001702.

15 G. Singh and P. K. Singh, *Langmuir*, 2019, **35**, 14628–14638.

16 T. Yorozu, M. Hoshino and M. Imamura, *J. Phys. Chem.*, 1982, **86**, 4426–4429.

17 C. Yang, W. Chen, X. Zhu, X. Song and M. Liu, *J. Phys. Chem. Lett.*, 2021, **12**, 7491–7496.

18 A. Harada and S.-i Nozakura, *Polym. Bull.*, 1982, **8**, 141–146.

19 M. V. Rekharsky, R. N. Goldberg, F. P. Schwarz, Y. B. Tewari, P. D. Ross, Y. Yamashoji and Y. Inoue, *J. Am. Chem. Soc.*, 1995, **117**, 8830–8840.

20 W. G. Herkstroeter, P. A. Martic and S. Farid, *J. Chem. Soc., Perkin Trans. 2*, 1984, 1453–1457, DOI: 10.1039/P29840001453.

21 X. Gao, Y. Wang, X. Wang, X. Guo, J. Huang and Y. Yan, *J. Mater. Chem. C*, 2017, **5**, 8936–8943.

22 K. Liu, S. Zang, R. Xue, J. Yang, L. Wang, J. Huang and Y. Yan, *ACS Appl. Mater. Interfaces*, 2018, **10**, 4530–4539.

23 Y. Qiao, Y. Lin, S. Liu, S. Zhang, H. Chen, Y. Wang, Y. Yan, X. Guo and J. Huang, *Chem. Commun.*, 2013, **49**, 704–706.

24 Y. Wang, X. Gao, Y. Xiao, Q. Zhao, J. Yang, Y. Yan and J. Huang, *Soft Matter*, 2015, **11**, 2806–2811.

25 M. Nara, H. Torii and M. Tasumi, *J. Phys. Chem.*, 1996, **100**, 19812–19817.

26 G. Deacon, *Coord. Chem. Rev.*, 1980, **33**, 227–250.

27 Y. Wang, X. Gao, Y. Xiao, Q. Zhao, J. Yang, Y. Yan and J. Huang, *Soft Matter*, 2015, **11**, 2806–2811.

28 C. K. Ober and G. Wegner, *Adv. Mater.*, 1997, **9**, 17–31.

29 Y. Kamikawa and T. Kato, *Langmuir*, 2007, **23** 274–278.